MOLECULAR AND CELLULAR BIOLOGY, July 1989, p. 2868–2880
0270-7306/89/072868-13$02.00/0

Vol. 9, No. 7

Nonsense Mutations in the Dihydrofolate Reductase Gene Affect RNA Processing

GAIL URLAUB, PAMELA J. MITCHELL, CARLOS J. CIUDAD, AND LAWRENCE A. CHASIN*
Department of Biological Sciences, Columbia University, New York, New York 10027

Received 31 January 1989/Accepted 30 March 1989

Steady-state dihydrofolate reductase (*dhfr*) mRNA levels were decreased as a result of nonsense mutations in the *dhfr* gene. Thirteen DHFR-deficient mutants were isolated after treatment of Chinese hamster ovary cells with UV irradiation. The positions of most point mutations were localized by RNA heteroduplex mapping, the mutated regions were isolated by cloning or by enzymatic amplification, and base changes were determined by DNA sequencing. Two of the mutants suffered large deletions that spanned the entire *dhfr* gene. The remaining 11 mutations consisted of nine single-base substitutions, one double-base substitution, and one single-base insertion. All of the single-base substitutions took place at the 3′ position of a pyrimidine dinucleotide, supporting the idea that UV mutagenesis proceeds through the formation of pyrimidine dimers in mammalian cells. Of the 11 point mutations, 10 resulted in nonsense codons, either directly or by a frameshift, suggesting that the selection method favored a null phenotype. An examination of steady-state RNA levels in cells carrying these mutations and a comparison with similar data from other *dhfr* mutants (A. M. Carothers, R. W. Steigerwalt, G. Urlaub, L. A. Chasin, and D. Grunberger, J. Mol. Biol., in press) showed that translation termination mutations in any of the internal exons of the gene gave rise to a low-RNA phenotype, whereas missense mutations in these exons or terminations in exon 6 (the final exon) did not affect *dhfr* mRNA levels. Nuclear run-on experiments showed that transcription of the mutant genes was normal. The stability of mature *dhfr* mRNA also was not affected, since (i) decay rates were the same in wild-type and mutant cells after inhibition of RNA synthesis with actinomycin D and (ii) intronless minigene versions of cloned wild-type and nonsense mutant genes were expressed equally after stable transfection. We conclude that RNA processing has been affected by these nonsense mutations and present a model in which both splicing and nuclear transport of an RNA molecule are coupled to its translation. Curiously, the low-RNA mutant phenotype was not exhibited after transfer of the mutant genes, suggesting that the transcripts of transfected genes may be processed differently than are those of their endogenous counterparts.

In an effort to identify and understand those aspects of gene structure that play a role in gene expression in mammalian cells, we have been carrying out a detailed mutational analysis of the dihydrofolate reductase (*dhfr*) gene in Chinese hamster ovary (CHO) cells. *dhfr* exhibits many typical characteristics of mammalian housekeeping genes: it is 25 kilobase pairs (kbp) in size, contains five variously sized introns, and has a promoter region with no TATA box but with a very high G+C content and an Sp1 binding site (10, 22, 40, 53). The basic strategy has been to isolate mutants that are deficient in DHFR enzyme activity; such mutants can be readily selected from a CHO cell line that is hemizygous at this locus (58, 59). To focus on lesions that may affect transcription or RNA processing, mutants can be screened for alterations that have affected *dhfr* mRNA, either qualitatively or quantitatively.

We have previously described spontaneous point mutations in the *dhfr* gene that inactivate splice sites and result in exon skipping (41). Although qualitatively altered, this aberrant mRNA is produced in normal amounts. In contrast, among point mutants induced with chemical carcinogens, we found many that accumulate only low levels of normally spliced *dhfr* mRNA (9, 12). Recent sequencing results revealed that all of these low-RNA mutants contain a premature translational termination codon caused by a nonsense or by a frameshift mutation. Nonsense mutations have previously been reported to decrease mRNA levels in bacteria (45), in yeasts (34), at the mouse immunoglobulin locus (5), and in the human β-globin (3, 4, 28, 42, 46, 54) and triose phosphate isomerase (TPI) genes (19).

In this study, we have characterized a series of mutations at the *dhfr* locus induced by UV irradiation of CHO cells. Most of the induced mutations were single-base substitutions that occurred at pyrimidine dimers. A high proportion of the mutations resulted in nonsense codons and the low-RNA phenotype. The low RNA levels in the mutants were shown not to be caused by low transcription rates or by the instability of mature mRNA. We conclude that RNA processing has been affected by mutations that interfere with translation or a translationlike process and present a model in which both splicing and nuclear transport of an RNA molecule are coupled to its translation.

MATERIALS AND METHODS

Cell culture and mutagenesis. The parental cell line used in this study was UA2, a derivative of CHO cells that is hemizygous for the *dhfr* gene (59). General methods of cell culture and methods for selection of DHFR-deficient mutants and their revertants have been previously described (58, 60). UV mutagenesis was performed by irradiating UA2 cells in three uncovered 100-mm-diameter dishes, each containing 1.7×10^7 cells in 8.5 ml of medium. Irradiation for 11 s 60 cm from a 30-W germicidal fluorescent lamp resulted in a survival of 10 to 20%. The cultures were immediately divided among 16 150-mm-diameter dishes. Each independent culture was then maintained in nonselective medium for expression of the DHFR-deficient phenotype; at least 10^6 cells were passaged as the cultures became confluent. After

* Corresponding author.

6 days, the cultures were subjected to selection by the tritiated deoxyuridine suicide method (58). Potential mutant colonies were cloned with cylinders, tested for purine auxotrophy characteristic of DHFR-deficient cells, and then recloned and maintained in nonselective medium or frozen. Only one mutant from each culture was chosen for further study, which ensured the independence of each mutant analyzed. DHFR was measured by [^{3}H]methotrexate binding (58).

Plasmid constructions and transfections. The construction of an intronless Chinese hamster *dhfr* minigene, pDCH0, has been described (62). A version carrying the nonsense mutation of mutant DU9 was constructed by cloning a 2.7-kbp *Eco*RI fragment spanning exon 3 from the cosmid pDU9 into pUC8 to yield pDU92E. From this plasmid, a 77-bp *Hpa*II-*Sst*I fragment from exon 3 that contained the DU9 mutation was used to mutagenize pDCH0 by a modified gapped-synthesis method (17, 32). The DU9 mutation has destroyed a *Taq*I site at cDNA position 196; the absence of this site made it possible to confirm the presence of the mutation in constructs and in transfectants. Transfections were carried out by the calcium phosphate coprecipitation method (63), using supercoiled plasmid or linearized (with *Sal*I) cosmid DNA for the stable-transfection experiments and supercoiled cosmid DNA for the transient-expression experiments. For the transfer of intronless *dhfr* minigenes, a DNA mixture consisting of 2 μg of the *dhfr* construct, 0.4 μg of pNEOBPV100 (36), and 17.6 μg of carrier calf thymus DNA per 10-cm-diameter tissue culture dish was used. For the transfer of cloned genomic genes, 1 μg of cosmid DNA (the vector for which contained the bacterial *neo* gene) and 19 μg of carrier were used. After 6 h of exposure to DNA and 24 h of expression in nonselective medium, transfectants that had received the *neo* gene were selected in 400 μg of active G418 (GIBCO Laboratories) per ml. Colonies were pooled, expanded in G418-containing medium, and then used for preparation of DNA and RNA.

RNA heteroduplex mapping of *dhfr* mutations. Total cellular RNA was prepared (14) and analyzed for mismatches in heteroduplexes with wild-type cRNA by cleaving with RNase under stringent hybridization conditions (44, 64). Three distinct riboprobes complementary to protein-coding regions of *dhfr* mRNA were used. These probes and the exact methodology have been described previously (9). Two of the riboprobes are shown in Fig. 1D.

RNA analysis. RNase protection analysis of *dhfr* and chloramphenicol acetyltransferase (CAT) mRNA was performed by the method of Melton et al. (39). Northern (RNA) blot hybridizations were carried out on poly(A)$^+$ RNA as described previously (40), using a mixture of two recombinant plasmid probes, pA3-A35 (38) and pMB5 (10). To measure the stability of *dhfr* mRNA, actinomycin D (5 μg/ml; Sigma Chemical Co.) was added to a 2.5-liter suspension culture of cells growing exponentially at a density of 3.5 × 10^5 to 6 × 10^5 cells per ml. After 0, 2, 4, 8, and 13 h, 200 to 500 ml of a culture was harvested; poly(A)$^+$ RNA was then prepared and subjected to Northern blot hybridization, using the two probes mentioned above plus a probe for the adenine phosphoribosyltransferase (*aprt*) gene as a positive control, as described previously (40). Filters were exposed to Kodak XAR-5 film (Eastman Kodak Co.) at −80°C, using a Lightning-Plus intensifying screen (E. I. du Pont de Nemours & Co., Inc.). After development, signal intensity was quantified with a densitometer (Bio-Rad Laboratories), correcting for film nonlinearity as described previously (47).

DNA analysis. The entire 25-kbp *dhfr* gene was analyzed in each of the 13 UV-induced mutants by Southern blot hybridization, using a mixture of 10 probes that span 35 kbp at this locus (11). Mutants DU5 and DU11 yielded no hybridization signal; their characterization as large deletions has been previously reported (61). The remaining 11 mutants yielded Southern hybridization patterns indistinguishable from that of the parental UA2 line (13) and were tentatively classified as point mutants.

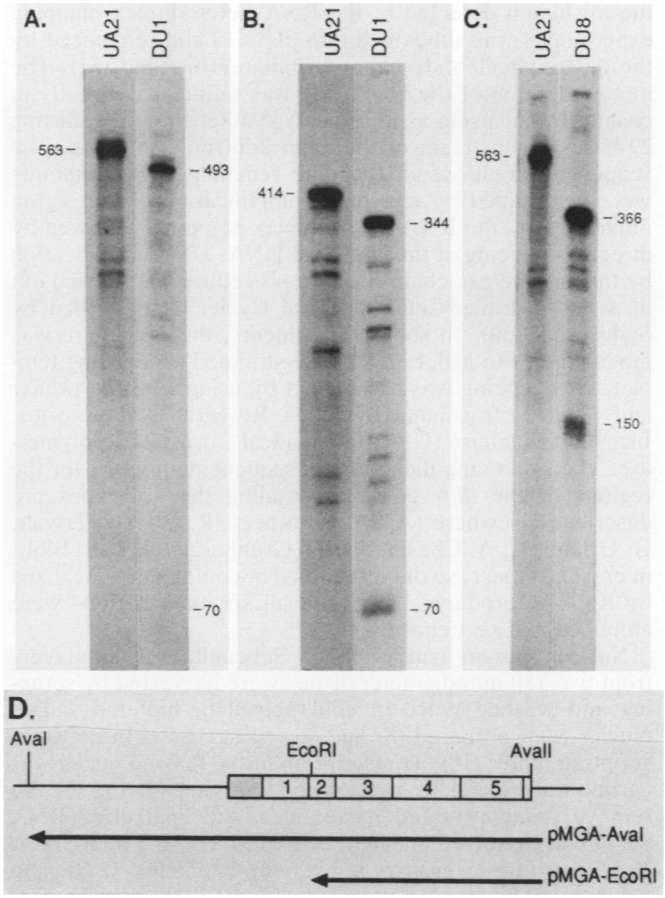

FIG. 1. RNA heteroduplex mapping of mutant RNA. Total cellular RNA from wild-type UA2 (10 μg), mutant DU1 (50 μg), or mutant DU8 (10 μg) was annealed to the riboprobe pMGA-AvaI (A and C) or pMGA-EcoRI (B), and then duplicate samples were treated with RNase. (D) cDNA sequence showing regions spanned by the riboprobes; thin lines represent either the 5′ genomic flank or 3′ vector sequences. The protected fragments were subjected to electrophoresis in denaturing 4% polyacrylamide gels. The markers (not shown) were end-labeled fragments of *Msp*I-digested pBR322 DNA. The predominant band at the top of the UA2 lanes represents protection of the entire mRNA complementary sequence present in the probe. Lower-molecular-weight bands in this lane represent minor homoduplex degradation products generated under these conditions. The sizes (in bases) of new predominant degradation products characteristic of each mutant heteroduplex are indicated. The low-molecular-weight band in the DU1 lane of panel A is visible on the original autoradiograph. The experiments were carried out under conditions of probe excess; therefore, the relative intensities of the bands are a measure of the *dhfr* mRNA content of each cell line.

Cloning mutant *dhfr* genes and gene fragments. The mutated *dhfr* genes of mutants DU8 and DU9 were cloned as 41-kbp inserts in a specialized cosmid vector designed for this purpose (57). The regions of the DU9 gene that harbored

the mismatch detected in the RNA heteroduplex mapping experiments was subcloned into pUC119 and sequenced by the dideoxynucleotide chain termination method (51). The mutated region of the DU8 gene was sequenced directly in cosmid DNA, using as a primer a synthetic 20-mer starting 29 bases downstream of the exon 2-intron 2 junction. The sequence alterations in the nine remaining point mutants were determined by enzymatic amplification of the region implicated by the RNA heteroduplex mapping, followed by direct sequencing of the amplified DNA. DNA amplification by the polymerase chain reaction procedure was carried out in a Perkin-Elmer-Cetus Thermal Cycler as described by Saiki et al. (50). In some experiments, the procedure was modified (25) to generate a single-stranded sequencing template. Sequencing was carried out by using a nested primer and Klenow fragment (Bethesda Research Laboratories, Inc.) or Sequenase (U.S. Biochemical Corp.) as a polymerase. The exact amplification and sequencing primers for the regions of the *dhfr* gene surrounding the six exons are described elsewhere (A. M. Carothers, R. W. Steigerwalt, G. Urlaub, L. A. Chasin, and D. Grunberger, J. Mol. Biol., in press). In the case of mutations that could not be localized by RNA heteroduplex mapping, all six exon regions were amplified and sequenced.

Nuclear run-on transcription. Subconfluent monolayers from two 150-mm-diameter dishes were harvested by scraping and washed twice in cold phosphate-buffered saline. Nuclei were prepared (8) and stored at −95°C in 2× transcription buffer (16). Transcription in the thawed nuclei was carried out essentially as described previously (16, 37). To remove unincorporated nucleotides, the final dried RNA pellet was dissolved in 300 μl of 10 mM Tris–0.1 mM EDTA and centrifuged through a prespun Sephadex G-50 spin column that had been pretreated with diethylpyrocarbonate. The eluate was adjusted to 0.25 M sodium acetate, and the RNA was precipitated with 2.5 volumes of ethanol. The ^{32}P-labeled RNA (4×10^7 to 6×10^7 cpm) was suspended in 100 μl of hybridization buffer containing 5× SSPE (1× SSPE is 180 mM NaCl, 10 mM NaH_2PO_4, and 1 mM EDTA [pH 6.4]), 5× Denhardt solution, 50% formamide, 1% sodium dodecyl sulfate (SDS), and 100 μg of tRNA per ml. For hybridization analysis of the labeled RNA, single-stranded DNA samples were immobilized on a GeneScreen Plus (Dupont, NEN Research Products) membrane, using a slot blotting manifold (Bethesda Research Laboratories) according to the instructions of the manufacturer. Each slot was further washed with 0.8 ml of 5× SSPE. The membranes were air dried for 15 min and baked at 80°C for the same period of time. Slots containing 2.5 and 5 μg of DNA yielded the same signal in the analysis of the transcription rate of CHO MK42 cells (200 *dhfr* copies), showing that the amount of DNA was in excess; 5 μg of DNA per slot was routinely used. Each membrane strip contained DNA from four sources. As a positive control, MT-5, a recombinant bacteriophage in M13mp19 containing a 3.8-kbp *Bam*HI fragment spanning the hamster *aprt* gene, was used. M13mp19 phage DNA served as a negative control. To detect *dhfr* sequences, we used an equimolar mixture of four recombinant phages carrying *dhfr* sequences, all in M13mp18 or M13mp19: MT-1, containing a 3.2-kbp sequence from intron 5; MT-2, containing a 1.7-kbp sequence from intron 3; MT-4, containing a 1.8-kbp sequence from intron 4; and ME-134, containing a 1.3-kbp *Eco*RI fragment spanning the 5′ flank through exon 2. The first three of these inserts are derived from the previously described (10) pBR322 clones pB67 (*Bam*HI-*Hin*dIII fragment), pB614 (*Bam*HI-*Sac*I fragment), and pB61 (*Hin*dIII fragment), respectively. The sequence of the ME-134 insert has been reported elsewhere (40). In total, these sequences represent 8.2-kbp of single-stranded *dhfr* DNA free of highly repeated sequences. We found that cloned *dhfr* cDNA could not be used as a probe, since it produced a high background signal when hybridized with ^{32}P-labeled transcripts isolated from a *dhfr*-negative deletion mutant. Finally, a reagent control with no DNA was included.

Membrane strips were prehybridized overnight at 42°C in 500 μl of hybridization buffer in a cylindrical plastic tube (10 by 35 mm). The tubes were rotated at 3 rpm at a 45° angle so that the small volume of hybridization solution would be constantly bathing the membrane. Hybridizations were started by addition of equal amounts the labeled probe in 100 μl of hybridization buffer and rotation at 42°C for 48 h. The filters were washed with 2× SSC (0.3 M NaCl plus 0.025 M sodium citrate, pH 7.0) twice for 5 min at room temperature, once with 2× SSC–1% SDS at 37°C for 60 min, and then with 0.1× SSC–1% SDS, 1% SDS, and 0.1× SSC, each at 65°C for 30 min. Wet washed hybridization membranes were processed for autoradiography as described above for RNA analysis. The amount of *dhfr*-specific transcription was calculated by normalizing the intensities of the *dhfr* bands to that for *aprt* after subtracting the M13 background.

RESULTS

Induction and isolation of DHFR-deficient mutants. The parental cell line used to generate DHFR-deficient mutants was the CHO derivative UA2. These cells are hemizygous at the *dhfr* locus, having suffered a deletion of one of the two *dhfr* alleles. Recessive mutations in which the remaining allele has been inactivated can be readily isolated by using a tritiated deoxyuridine suicide technique. DHFR-deficient mutants cannot incorporate this precursor into DNA and are selected (58). UV irradiation was an efficient mutagen for producing DHFR-deficient mutants. At doses that killed 80 to 90% of the treated UA2 cells, DHFR-deficient mutants were induced at an average frequency of 8.5×10^{-5}. Thirteen mutants were recloned for further analysis. All displayed the triple auxotrophy characteristic of tetrahydrofolate-deprived cells: unlike the parental cells, they required glycine, a purine (e.g., hypoxanthine), and thymidine for growth. DHFR activity was undetectable in extracts prepared from mutants, indicating a decrease to less than 1 to 2% of the parental enzyme level.

Mapping the mutations induced by UV. To determine the DNA sequence changes brought about by these mutations, we first examined mutant DNA for evidence of gross lesions (deletions or disruptions) in the 25-kbp *dhfr* gene. After digestion with *Kpn*I and *Bst*EII, mutant DNA was subjected to Southern analysis, using a mixture of 10 probes that detects fragments spanning 35 kbp of contiguous DNA at the *dhfr* locus (11). Two mutants contained no DNA from this region and thus represented deletions of at least 35 kbp. The deletions in these two mutants, DU5 and DU11, were subsequently shown to be at least 95 and 200 kbp long, respectively (61). The remaining 11 mutants exhibited fragment patterns indistinguishable from that of the parental UA2 cells and so must have resulted from single-base changes, small deletions, or gene inactivation. The *dhfr* gene in CHO cells is methylated at CpG dinucleotides (shown for those amenable to restriction enzyme analysis) over most of its 25-kbp length, but a 4-kbp region that straddles the transcription start site is free of such modification (40). A similar analysis was carried out for eight of the UV-induced

TABLE 1. Characteristics of UV-induced DHFR-deficient mutants

Mutation	Mutant	Level of:		Exon[c]	Position(s)[d]	Base changes[e]	Coding change[f]
		DHFR[a]	*dhfr* RNA[b]				
Wild type	UA21	100	100	NA	NA		
1	DU15	<1	10	1 (R)	86	G/G → G<u>A</u>/G	Frameshift → ochre-46
2	DU6	<1	8	2 (R)	106	C<u>C</u> → C<u>T</u>	Gln → ochre-35
3	DU8	<1	78	2 (R)	136, +1	<u>G/GT</u> → <u>A/A</u>T	Exon 2 skipped
4	DU9	<1	6	3	196	T<u>C</u> → T<u>T</u>	Arg → opal-65
5	DU12	<2	14	3	196	T<u>C</u> → T<u>T</u>	Arg → opal-65
6	DU2	<1	30	3 (R)	200	C<u>C</u> → C<u>T</u>	Pro →Leu-66
7	DU3	<1	16	5 (R)	382	T<u>C</u> → T<u>T</u>	Gln → amber-127
8	DU14	<1	10	5 (R)	382	T<u>C</u> → T<u>T</u>	Gln → amber-127
9	DU1	<1	20	5 (R)	430	<u>G</u>A → <u>T</u>A	Glu → ochre-143
10	DU4	<1	145	6	511	C<u>C</u> → C<u>T</u>	Gln → amber-170
11	DU16	<1	107	6 (R)	520	<u>A</u>A → <u>T</u>A	Lys → ochre-173
12	DU5	<1	<2	Entire gene deleted			
13	DU11	<1	<2	Entire gene deleted			

[a] Percentage of the DHFR-specific methotrexate-binding activity of the parental UA21 cells, which was 2 pmol/mg of soluble protein.
[b] From densitometric measurements of Northern analysis of total cellular poly(A)$^+$ RNA, with the results expressed as a percentage of the value for UA21 as measured on the same gel.
[c] The exon in which the mutation is located. NA, Not applicable; (R), mismatch detected by RNA heteroduplex mapping.
[d] Nucleotide base number in the cDNA. The A of the ATG translation initiation codon is 1, as in reference 39. For mutations in introns, the offset from the nearest exon border is given. NA, Not applicable.
[e] Refers to the protein-coding (nontemplate) strand. The mutated nucleotide is underlined. A slash denotes an exon-intron joint.
[f] Numbers indicate amino acid positions.

mutants (DU1, -2, -3, -6, -9, -12, -14, and -15). All exhibited methylation patterns indistinguishable from that of the parental UA2 cells (data not shown). Thus, there was no evidence that the lack of DHFR activity in these mutants was due to this type of gene inactivation.

We used the RNA-RNA heteroduplex mapping of Winter et al. (64) to map the positions of putative point mutations that had occurred in exons or caused splicing defects. In this procedure, a heteroduplex is formed between RNA from a mutant and a uniformly labeled riboprobe complementary to wild-type *dhfr* mRNA. Treatment with RNase results in preferential cleavage at the site of mismatched bases (Fig. 1A). Use of a second probe of different size allows the size of the mismatch to be pinpointed (Fig. 1B). In the case of a splicing defect (Fig. 1C), the lack of an exon in the mutant RNA produces efficient cleavage of the probe; the extent of the missing exonic sequence can be calculated from the summed sizes of the two fragments produced. The positions of mismatched bases in 8 of the 11 putative point mutants examined were revealed by the application of this technique. Three of the mutants (no. 4, 9, and 12) yielded no convincing evidence of a mismatch. This proportion is not unexpected, since RNase A will not cleave all single-stranded sequences.

Base changes in the UV-induced mutants. We next sought to determine the exact base changes associated with these mutations. In early experiments, we cloned the entire mutant gene as a 41-kbp insert in a custom cosmid vector designed to enrich for the *dhfr* gene (57). We then subcloned a smaller region, chosen on the basis of the RNA heteroduplex mapping results, into a pUC vector for sequencing. The mutated *dhfr* genes of DU8 and DU9 were cloned in this manner. In later experiments, we used the polymerase chain reaction method (50) to amplify a region of 150 to 300 bp spanning the site of the mismatch detected by the RNA heteroduplex mapping. This amplified DNA was then sequenced directly. In the three cases in which no mismatch was detected, we amplified and sequenced each of the six exons (together with intron flanks). The results of these sequence analyses are shown in Table 1. Ten of the eleven mutations were single-base changes; the exception (no. 3) was a double-base change involving two adjacent bases. All 11 mutations occurred within the protein-coding sequence of the gene and were distributed among all but one of the six exons of the gene. Two pairs of mutations (no. 4 and 5 and no. 7 and 8) had effected the same base change. Most (10 of 11) of the base changes occurred as eight transitions or two transversions at the second base of a pyrimidine dinucleotide, supporting the idea that they originated from pyrimidine dimer formation. One mutation (no. 1) was a single-base insertion rather than a base substitution. An unexpected finding was that the majority of the mutations resulted in nonsense codons. It may be that the selection method used was so stringent as to preclude the isolation of most missense mutants.

A splicing mutation causing exon 2 to be skipped. RNA heteroduplex analysis of mutant DU8 showed that this RNA contained a deletion of approximately 50 bases, from about position 90 to position 140 (the translational start being +1) in the mRNA (Fig. 1C, lane DU8). This region corresponds to exon 2, which suggests that exon 1 is spliced to exon 3 in this RNA. DNA sequencing results showed that the mutation in DU8 (no. 3) indeed affected a splice site: the two guanine residues that normally span the exon 2-intron 2 border had been changed to two adenines by a double-transition mutation (see reference 40 for the wild-type sequence). The mutation of the universally conserved guanine at the start of intron 2 is expected to eliminate splicing at this site. The inability to correctly splice intron 2 somehow affected the splicing of intron 1 as well. Rather than form a splice to the unmutated 5′ end of exon 2, exon 1 was spliced to exon 3. Exon 2 was treated as part of a larger intron and was skipped altogether. We have previously reported exon-skipping mutations in the case of exon 5 in the CHO *dhfr* gene (41). The phenotype of mutant DU8 shows that this response was not limited to a particular exon. Despite the unusual splicing pattern, a near-normal amount of *dhfr* mRNA was found in DU8 cells.

Mutants with low levels of *dhfr* mRNA. In addition to

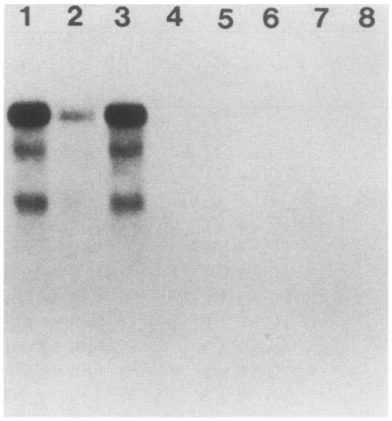

FIG. 2. Northern blot hybridization of mutant RNA. Poly(A)$^+$ (12 μg) or poly(A)$^-$ (24 μg) RNA was isolated from total cellular RNA, and electrophoresed in formaldehyde-agarose gels, and subjected to blot hybridization with the *dhfr* cDNA clone pA3-A35. The three molecular-size species of *dhfr* mRNA are the result of multiple polyadenylation sites. After exposure of the autoradiograms, the filters were dehybridized and rehybridized to a probe detecting *aprt* mRNA; the band intensities with this probe were equivalent in all lanes (not shown). Lanes: 1 and 5, UA2 (wild type); 2 and 6, DU1, a low-RNA mutant; 3 and 7, DU4, a normal-RNA mutant; 4 and 8, DU11, a *dhfr* deletion mutant. Lanes 1 to 4 contained poly(A)$^+$ RNA; lanes 5 to 8 contained poly(A)$^-$ RNA.

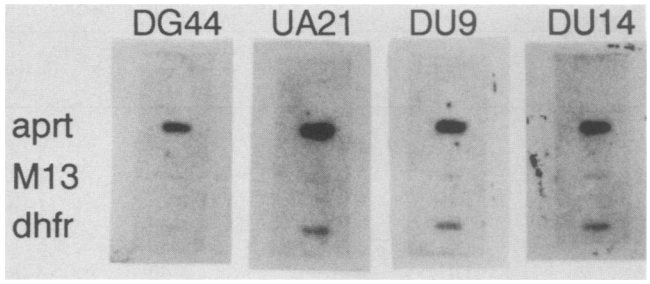

FIG. 3. Transcription of the *dhfr* gene in nuclei from mutant cells. Nuclei were prepared from the indicated UV-induced mutants as well as from the wild-type line UA2 and the double-deletion mutant DG44, which contains no *dhfr* genes. After 12 min of incorporation of [^{32}P]UTP, the labeled RNA was isolated and hybridized to a nylon filter strip containing three bands of DNA that had been applied in a slot blotting apparatus. The bottom band in each strip contained an excess (5 μg) of single-stranded DNA representing 8 kb of *dhfr* gene sequences free of highly repeated sequences. The middle band contained an equal amount of phage M13 DNA, the vector carrying the single-stranded *dhfr* probe sequences, as a negative control. The top band contained an equal amount of recombinant M13 carrying the 3-kb *aprt* gene as a positive control. Note the absence of a background signal for *dhfr* transcription in the strip hybridized to RNA from a *dhfr* deletion mutant, DG44 (61).

indicating the position of mismatched bases, the RNA heteroduplex mapping procedure provided a measure of the steady-state level of *dhfr* RNA in a mutant cell (e.g., see Fig. 5). Surprisingly, about two-thirds of the UV-induced mutants analyzed exhibited a dramatically decreased steady-state level of *dhfr* RNA (less than one-fifth of the parental level). Mutant *dhfr* mRNA levels were also quantified by densitometric analysis of Northern blot hybridizations of total poly(A)$^+$ RNA. An example is shown in Fig. 2, and the quantitative results for all 11 point mutants are presented in Table 1. We have found a similar proportion of mutants with low levels of *dhfr* RNA among those induced by benz[*a*]pyrene diol epoxide (9) and *N*-acetoxy-*N*-acetylaminofluorene (11, 12). Thus, this phenotype is not specific for UV mutagenesis.

***dhfr* transcription rates and mRNA stability in low-level mRNA mutants.** What is the cause of the dramatic decrease in steady-state *dhfr* mRNA in these mutants? A decreased rate of transcription seemed unlikely, since low-level mRNA mutations were scattered among many exons, and transcriptional control regions are typically clustered in flanks or introns. We nevertheless tested this possibility by run-on transcription assays in isolated nuclei. *dhfr* is not a highly transcribed gene; the steady-state level of *dhfr* mRNA in the parental UA2 cells is only about 10 to 20 copies per cell. To measure low levels of transcription, we used long regions (8.2 kbp) of immobilized single-stranded probes for slot hybridization. Transcription rates for the low-RNA mutants DU9 and DU14 were indistinguishable from that of the parental UA2 cells, the signals being at least severalfold higher than the background measurements obtained by using nuclei from a *dhfr* deletion mutant (Fig. 3).

The low level of *dhfr* RNA in these mutants could have been caused by an increased rate of degradation of the mature mRNA. This idea was tested by comparing the half-life of *dhfr* mRNA in a mutant and in the parental cell line after inhibition of new RNA synthesis with actinomycin D. The relative amounts of *dhfr* mRNA in the treated cultures were quantified by densitometric measurements of Northern blots of RNA samples prepared at various times after actinomycin D addition. For this experiment, mutant DU9 was chosen; this mutant contains 5 to 7% of the parental *dhfr* mRNA level, and it is one of those found to have a wild-type transcription rate, as described above. The residual *dhfr* mRNA of the DU9 mutant decayed at the same rate as in the parental UA2 cells, with a half-life of approximately 7.5 (Fig. 4). A similar result was obtained with mutant DU6 (data not shown). We conclude that lability of mature *dhfr* mRNA is not the cause of its low steady-state level, at least in these mutants. This conclusion must be qualified by the possibility that the interruption of RNA synthesis by actinomycin D interferes with the process that destabilizes the mRNA. The fact that the measured half-life of 7.5 h agrees well with previous determinations of the decay rate of mouse *dhfr* mRNA (measured in amplified cell lines without the use of drugs [27]) argues against an actinomycin-induced artifact here. Moreover, gene transfer experiments (see below) provided independent confirmation of the conclusion that mRNA stability was not involved.

Low-RNA mutants are the result of nonsense mutations. Of the five different base changes that led to a low-RNA phenotype, four were nonsense mutations and the fifth (Table 1, no. 1) was a single-base insertion that led to a downstream nonsense mutation. Thus, all of the low-RNA mutants involved nonsense mutations. However, not all nonsense mutations led to a low-RNA phenotype. Notably, the two nonsense mutations in exon 6 (no. 10 and 11) did not decrease *dhfr* RNA levels.

This correlation between a nonsense mutation and a low-RNA phenotype was further tested by reversion analysis of several low-RNA mutants. Although unlikely on statistical grounds, it is possible that a mutation in the *dhfr* gene other than the nonsense mutation was responsible for the low-mRNA phenotype. DU1, DU6, and DU9 cells were treated with ethyl methanesulfonate, and revertants capable of growth in a medium lacking purines were isolated. Rever-

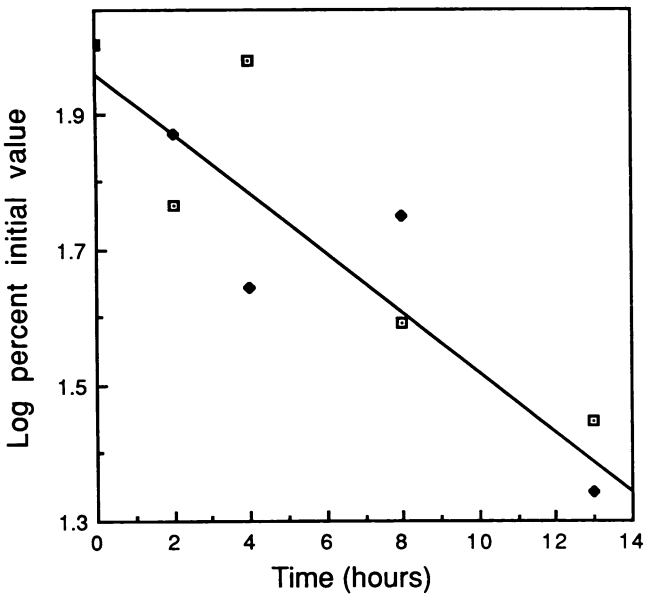

FIG. 4. Degradation rate of *dhfr* mRNA in wild-type (⊡) and mutant (◆) cells. Actinomycin D (5 μg/ml) was added to a suspension culture of wild-type (UA2) cells and to a parallel culture of DU9, a low-RNA nonsense mutant. At the indicated times, a sample of cells was removed, and poly(A)$^+$ was isolated and analyzed for *dhfr* mRNA by Northern hybridization as described in the legend to Fig. 2. The amount of the highest-molecular-weight mRNA species was quantified by densitometry and is expressed as the amount per unit volume of culture relative to the initial value. The absolute initial value for DU9 was 7% of that for UA2 in this experiment.

sion frequencies were low, in the range of 10^{-6}. All revertants tested grew well in a medium lacking glycine, purines, and thymidine. Analysis of six revertants showed true reversion to the wild-type sequence as well as further base substitution at the mutated site to produce an acceptable missense or a neutral codon (Table 2). *dhfr* mRNA levels were greatly increased in the revertants tested (Table 2), as shown for two wild-type DU9 revertants in Fig. 5. In the case of DU6, all four possible bases were represented at position 106; only T at that position (the nonsense mutation) yielded the low-RNA phenotype (Table 2). We conclude that the nonsense mutations alone at these positions are both necessary and sufficient to generate the low-mRNA phenotype.

There was also some evidence of a partial splicing defect in mutant DU9 (Fig. 5, lane 1). Whereas the major protected RNA species was the fully spliced mRNA, another protected fragment corresponding to exons 4 to 6 was generated by using this probe and other probes (data not shown), which suggested that exon 3-exon 4 splicing was defective. Curiously, the corresponding 5′ fragment, consisting of exons 1 to 3, was not present. These results suggest that DU9 cells are partially defective in splicing intron 3. The exon 4 region of DU9 DNA was sequenced and found to be wild type, and true revertants of DU9 regained wild-type splicing (Fig. 5). Thus, the data point to a splicing aberration caused by a nonsense mutation in exon 3 that was 46 bases upstream of the donor splice site.

Loss of the relative low-mRNA phenotype upon transfer of mutant minigenes. The only known consequence of nonsense mutations is on translation, and mature mRNA is the predominant translated species. The striking correlation between nonsense mutations and the low-RNA phenotype led us to reconsider the possibility that these nonsense mutations were destabilizing mature *dhfr* mRNA. We tested this idea further by analyzing *dhfr* RNA levels after gene transfer. An intronless minigene version of the mutated gene of DU9 was constructed by cloning the region of exon 3 containing the nonsense mutation into a CHO *dhfr* minigene. The wild-type intronless minigene has been previously described (62). It consists of hamster *dhfr* cDNA bounded by 800 bp of genomic sequence at the 5′ end (including the *dhfr* promoter) and 3′ sequences that include the first major polyadenylation site in exon 6. In parallel experiments, DNA from the wild-type and mutant versions of this minigene were used to transfect CHO DG44 cells, a double-deletion DHFR-deficient mutant that contains no *dhfr* genes (61). A plasmid carrying the bacterial *neo* gene was cotransfected along with the *dhfr* constructs, and hundreds of resulting G418-resistant colonies were pooled for RNA analysis by RNase protection. *dhfr* DNA in these pooled populations was quantified by Southern hybridization to correct the RNA levels for the average copy number of the transferred *dhfr* genes. If the 10- to 20-fold decrease in *dhfr* mRNA level in DU9 cells was due to mRNA instability, then the cells that received the mutant version of the minigene should have exhibited a lower steady-state level of RNA than did the cells transfected with the wild-type construct. No difference in *dhfr* RNA level per *dhfr* copy between the wild-type and mutant genes was found (Fig. 6). Therefore, mRNA stability cannot underlie the low-RNA phenotype, in agreement with results of the actinomycin D experiments.

The level of *dhfr* RNA per gene was lower in these transfected populations than in cells carrying a single copy of the endogenous *dhfr* gene (i.e., UA2 cells): as determined by

TABLE 2. Revertants of low-RNA nonsense mutants

Revertant	Position	Parent	Base changes[a]	Coding changes	*dhfr* mRNA level[b]
RDU6-1	106	DU6	CAA → TAA → AAA	Gln → ochre → Lys	83
RDU6-2	106	DU6	CAA → TAA → GAA	Gln → ochre → Glu	89
RDU9-1	196	DU9	CGA → TGA → CGA[c]	Arg → opal → Arg	106
RDU9-2	196	DU9	CGA → TGA → CGA[c]	Arg → opal → Arg	192
RDU9-3	196	DU9	CGA → TGA → CGA[c]	Arg → opal → Arg	44
RDU9-4	196	DU9	CGA → TGA → CGA[c]	Arg → opal → Arg	90
RDU9-5	196	DU9	CGA → TGA → AGA	Arg → opal → Arg	ND
RDU1-1	430	DU1	GAA → TAA → CAA	Glu → ochre → Gln	ND

[a] Wild type → mutant → revertant.
[b] Densitometric values from RNase protection experiments, expressed as a percentage of the value for the parental UA2 cells measured on the same gel. ND, Not determined.
[c] Sequence deduced from the fact that the wild-type *Taq*I site was restored.

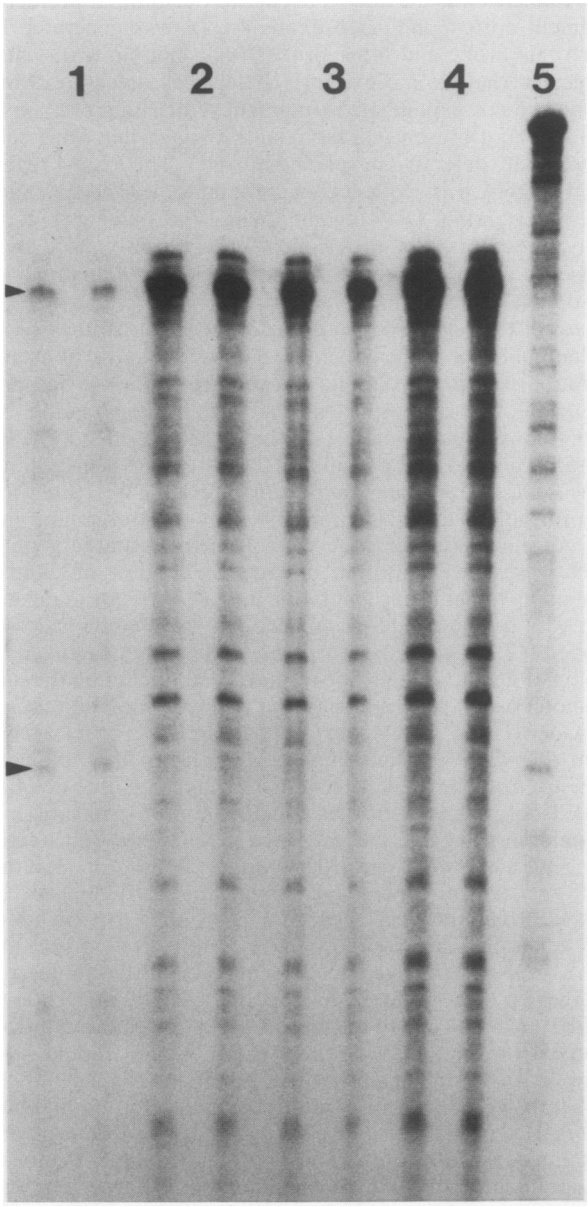

FIG. 5. Quantitation of *dhfr* mRNA in a nonsense mutant and its revertants. Total cellular RNA from mutant DU9 and from two revertants, as well as from wild-type UA2 cells, was annealed to an excess of riboprobe pMGA-AvaI (see legend to Fig. 1) and subjected to RNase protection analysis. Duplicate lanes: 1, DU9 RNA; 2, UA2; 3, revertant RDU9-1; 4, revertant RDU9-2; 5, undigested riboprobe. For lanes 1, 30 μg of RNA was used; 10 μg was used for all other lanes. The upper arrowhead indicates the position of the protected fragment expected from spliced *dhfr* transcripts (563 bases); the lower arrowhead indicates a second protected fragment of 258 bases seen in lane 1, which corresponds in size to the exon 4, 5, and 6 portions of the probe; a fragment of this size would arise from the failure to splice exon 3 to exon 4. Markers were end-labeled *Msp*I-digested pBR322 DNA (not shown).

densitometric comparisons in the RNase protection experiments, the transfected populations contained about 1% of the *dhfr* RNA of UA2 cells on a per-gene-copy-number basis. Poor expression of intronless *dhfr* genes has been noted previously (7, 18, 23, 62).

Loss of the relative low-RNA phenotype upon transfer of mutant genomic genes. The elimination of transcription and mRNA stability as possible causes of the low-RNA phenotype leaves transcript processing as the affected step. Since the removal of introns in construction of the minigenes abolished the effect, splicing is suggested as at least one of the processing operations affected. A possible test of this idea was to repeat the gene transfer experiment with the introns in place. We therefore performed the same parallel transfections of DG44 cells, using cosmid clones carrying either the wild-type *dhfr* gene (pD35) or the mutated *dhfr* gene of DU9 (pDU9). Both cosmids contain a 25-kbp *dhfr* gene approximately centrally located within a 41-kbp insert. Since they also contain a *neo* gene as part of the plasmid, transfectants could be directly selected on the basis of G418 resistance. Drug-resistant colonies were again pooled and assayed for *dhfr* mRNA and DNA. If intron removal was the only important factor in expression of the low-RNA phenotype of mutant DU9, then the pDU9-transfected cells should have exhibited a 10-fold lower value of RNA per gene copy. Much to our surprise, the transfected genomic genes again failed to reproduce the phenotype of their endogenous counterparts: populations transfected by the wild-type or the mutated genomic genes expressed the same level of *dhfr* RNA (Fig. 6). This level was considerably higher than that yielded by the intronless minigenes, which suggested that introns aided in gene expression. However, it should be noted that although the transfected genomic genes were expressed more efficiently than their minigene counterparts, they still produced much less RNA than did an endogenous *dhfr* gene (4.5% of the level of UA2 cells on a per-gene-copy-number basis). We also tested the expression of the low-RNA mutant phenotype of the genomic genes in a transient-expression experiment. Supercoiled wild-type (pD35) or mutant (pDU9) cosmid DNA was transfected into DG44 cells along with a plasmid containing the CAT gene driven by a simian virus 40 promoter-enhancer. RNA was isolated 48 h posttransfection and analyzed for *dhfr* RNA and CAT RNA by RNase protection; the CAT RNA values showed that transfection efficiencies were the same in the two cases. Once again, no difference was found between the wild-type and mutant genes in the level of *dhfr* RNA produced (data not shown). Expression of the low-RNA phenotype apparently depended not (or not just) on the simple inclusion of introns but may have involved factors that differ between the endogenous and exogenous genes, such as position within the nucleus, methylation status, or extent of distant flanking sequences.

DISCUSSION

UV mutagenesis. Sequence analysis of the point mutations induced by UV irradiation confirms the idea that the principal mutagenic lesion induced by UV is a pyrimidine dimer. In all 11 point mutations, a change occurred at the 3′ pyrimidine of a pyrimidine dinucleotide. The presumed target pyrimidine dinucleotides are approximately equally represented on the coding and noncoding strands of the DNA. Despite the predominance of thymine dimers in UV-treated cells (26), in all but one case the 3′ base of the target dinucleotide was a cytosine. This selectivity was not caused by the bias of the selective system toward nonsense mutations: of the possible pyrimidine dinucleotides that can give rise to a nonsense codon by a single-base substitution at the 3′ position, 46% are TT or CT, yet a 3′ T was the target in only one (DU16) of the eight nonsense mutants analyzed. We conclude that the CC and TC dimers are the most

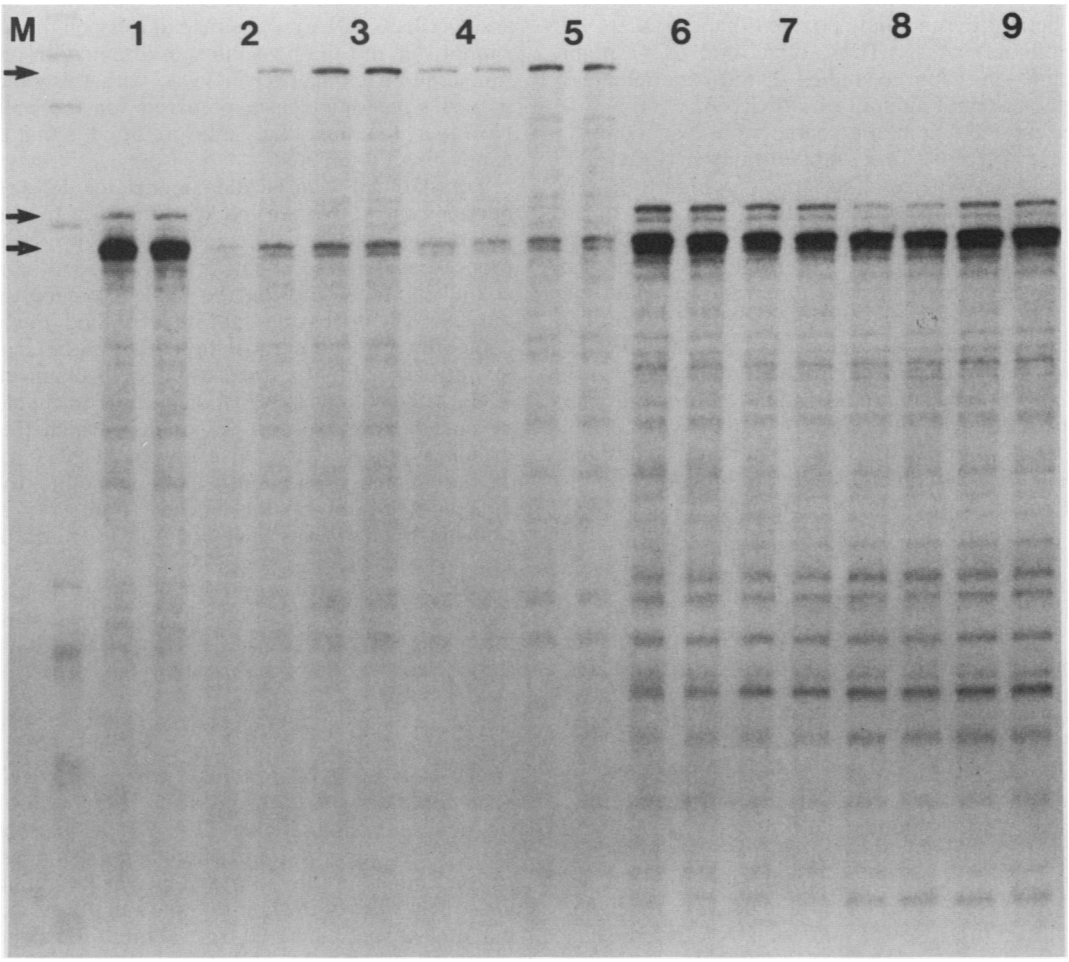

FIG. 6. Quantitation of *dhfr* mRNA levels in cells transfected with wild-type or mutant genes. Cells of the double-deletion mutant DG44 were cotransfected with pNEOBPV100 DNA plus DNA from a wild-type intronless *dhfr* minigene, pDCH0 (lanes 2 and 3); pNEOBPV100 DNA plus DNA from a similar minigene construct (pDCH9) carrying the nonsense mutation of mutant DU9 in exon 3 (lanes 4 and 5); DNA of cosmid pD35, carrying the wild-type *dhfr* genomic gene (lanes 6 and 7); or DNA from cosmid pDU9, carrying the genomic gene cloned from mutant DU9 (lanes 8 and 9). In the case of the cosmids, resistance to G418 was conferred by a *neo* gene in the vector. Hundreds of G418-resistant transfectant colonies were pooled, expanded, and used for preparation of total cellular DNA and RNA. The *dhfr* gene copy number of these populations was determined by quantitation of Southern hybridizations (see below). The RNA was annealed to the riboprobe pMGA-AvaI, and samples of 30 (lanes 2 to 5) or 10 μg were analyzed in duplicate by RNase protection. Note that both wild-type and mutant mRNAs yielded full-length protected fragments since this combination of mismatched bases in the heteroduplex was not recognized by RNase (see also Fig. 5). Lanes: M, markers of end-labeled *Msp*I-digested pBR322 DNA; 1, digestion products of 10 μg of UA2 RNA (1 gene copy per cell); 2 and 3, DCH0-1 (13 gene copies per cell) and DCH0-2 (15 copies), two independent populations transfected with the wild-type minigene; 4 and 5, DCH9-1 (4 copies) and DCH9-2 (5 copies), two independent populations transfected with a minigene harboring the nonsense mutation of DU9; 6 and 7, G1 (13 copies) and G2 (14 copies), two independent populations transfected with DNA from the wild-type cosmid pD35; 8 and 9, G3 (13 copies) and G4 (24 copies), two independent populations transfected with DNA from the cosmid pDU9, carrying the mutant gene. The bottom arrow points to the position of the fully protected mRNA portion of the probe; the middle arrow points to the spliced RNA originating at a minor upstream promoter; and the top arrow points to the position of transcripts originating from a cryptic upstream promoter, probably in the vector (15).

important premutagenic lesions in UV-treated mammalian cells, as was also the case in the analysis of the *aprt* locus in Chinese hamster cells (20) and in exogenous genes introduced into mammalian cells by shuttle vectors (24, 26, 33).

Mutations that cause exon skipping. In the β-thalassemias, the mutational destruction of a splice site often results in the activation of a nearly cryptic site. In contrast, exon skipping is the more frequent consequence in the *dhfr* gene. Inactivation of the intron 2 donor splice site in mutant DU8 represents a new example of exon skipping in the *dhfr* gene; we have previously described this phenomenon for exon 5 (41). The ready skipping of exons in the *dhfr* mutants also contrasts with the suggestion that exon skipping is less likely to occur in vivo than in a cell-free splicing system (1). This idea was based on the analysis of site-directed mutations in the rabbit β-globin gene: mutant RNA molecules that skipped exons in a cell-free splicing system did not skip them in transfected cells (1). The possibility must be considered that transcripts of transfected genes behave differently from their in situ as well as their in vitro counterparts (see below).

Nonsense mutations affect RNA processing. Our survey of RNA phenotypes of DHFR-deficient mutants has shown that many exhibit much reduced steady-state levels of *dhfr* RNA. This finding holds not only for the UV-induced mutants

described here but also for mutants induced by two chemical carcinogens, benz[*a*]pyrene diol epoxide (9) and *N*-acetoxy-*N*-acetylaminofluorene (11). Thus, of a total of 41 point mutants examined in the three studies, 23 (56%) contain less than 20% of the parental amount of *dhfr* RNA.

All of the low-RNA mutants carry nonsense codons, either created directly by base substitutions or generated indirectly by frameshifts or abnormal splicing. It is the nonsense codon and not some additional mutation in an unsequenced region of this large gene that is responsible for the low-RNA phenotype, since revertants in which the nonsense codon is restored to wild type recover wild-type RNA levels. The evidence suggests that it is a functional consequence of the nonsense codons and not a change in RNA structure that is responsible for the low-RNA phenotype: none of six missense mutants produces this phenotype, and revertants of low RNA nonsense mutants regain normal RNA levels even when they do not restore the wild-type sequence (i.e., they become acceptable missense mutations). Furthermore, more extreme changes in nucleotide sequence represented by deletions do not bring about the low-RNA phenotype. A mutant with a deletion that spans exon 5 (DF20; 11) produces wild-type levels of RNA (12), as do splicing mutants that skip exon 2 (DU8), exon 5, or exons 4 plus 5 (41). Finally, it is unlikely that nonsense codons act through secondary structure when they have been generated by a frameshift that is located 50 bases upstream. In these cases, the nonsense codon is in the context of an unchanged wild-type sequence.

In the work described here, we examined the level at which the reduction of RNA takes place. For much of this characterization, we used mutant DU9 as a prototype. The mutation in DU9 is a C-to-T transition near the center of *dhfr* exon 3; it results in an opal chain termination codon. Low steady-state RNA levels could have three causes: (i) a lower transcription rate; (ii) a lower rate of RNA processing, coupled with the rapid destruction of an unstable processing intermediate; and (iii) unstable mature mRNA. The fact that all of the low-RNA mutants involve nonsense codons suggested mRNA stability as the determinant most likely affected. After all, nonsense codons modify translation, and it is the mature mRNA that is the principal substrate for translation. Moreover, nonsense mutations have been reported to affect mRNA stability in *Escherichia coli* (45) and yeast cells (34). In mammalian cells, it is known that mRNA stability can be influenced by the nascent polypeptide, as in the case of tubulin (48), or by RNA secondary structure, as in histone mRNA (49). However, the results of our experiments argue strongly against mature mRNA lability in these mutants. First, after new RNA synthesis was stopped by treatment with actinomycin D, the subsequent rates of decay of *dhfr* mRNA were the same in mutant and wild-type cells. Second, in stable-transfection experiments, cells that received a mutant cDNA-based *dhfr* minigene containing the same nonsense mutation as did DU9 produced the same amount of RNA as did those that received a wild-type version. If the low-RNA levels were due to an instability imparted by an altered base in the RNA, then the mutant minigene should have reproduced the low-RNA phenotype. These two experiments rule out straightforward explanations based on mRNA stability.

It seemed less likely that these nonsense mutations affect transcription, since translation and transcription take place in two different cellular compartments in eucaryotic cells. Nonetheless, this idea was tested by in vitro nuclear run-on transcription assays, and once again the low-RNA mutants showed no difference from wild-type parental cells. This assay reflects RNA polymerase density on the *dhfr* gene; we cannot rule out the possibility of attenuation or blocking of transcription elongation in vivo, with this block being removed when nuclei are prepared for the in vitro assay. However, the most likely interpretation is that transcription is not directly affected.

Translational translocation model for RNA splicing and nuclear export. We are left with the idea that a step in the processing of RNA is affected by nonsense mutations. One processing step, the export of mRNA from the nucleus, lies at the interface between the nuclear compartment, where most RNA processing takes place, and the cytoplasmic compartment, where translation takes place. Indeed, Zasloff (65) has argued that a translationlike mechanism is involved in the transport of tRNA molecules from nucleus to cytoplasm. Our data suggest a model in which the process of protein synthesis itself pulls translatable RNA molecules out of the nucleus. The most likely conduits for the RNA molecules would be the nuclear pores (6, 21). Indeed, ribosomelike particles have been observed on the cytoplasmic face of nuclear pores (56). When translation becomes stalled because a ribosome encounters a nonsense codon, the pulling stops, RNA transport is slowed considerably, and the nuclear portion of each RNA molecule is vulnerable to the nuclear enzymes that destroy most heterogeneous nuclear RNA.

There are two related facts that are not consistent with this translational translocation model as it stands. First, the model does not explain why a wild-type mRNA molecule does not stall when ribosomes reach the natural translation termination codon. Many mRNA molecules have long 3′ untranslated regions, *dhfr* being a good example. The termination codon for the shortest species of Chinese hamster *dhfr* mRNA lies at the halfway mark in the molecule, and for the longest species (2,400 bases), three-fourths of the molecule lies beyond the termination codon (10, 38). Thus, these wild-type molecules should be subject to nearly the same nuclear destruction as are nonsense mutants. Second, not all nonsense mutations in the *dhfr* gene result in a low-RNA phenotype. The factor that determines the low-RNA phenotype is the position of the mutation. Figure 7A presents the mutation positions and RNA levels from 36 *dhfr* mutants whose sequences have been determined in this and two other studies (41; Carothers et al., J. Mol. Biol., in press). In Fig. 7B, the missense mutations, with their high RNA levels, have been removed; the 24 nonsense and nonsense-generating frameshift and splicing mutations tend to yield high RNA levels when they occur toward the 3′ end of the gene. This bias becomes even clearer if the positions of the generated nonsense codons, rather than the mutations themselves, are considered. The low-RNA phenotype now exhibits a striking relationship with respect to the position of the nonsense codons: chain terminations occurring in exon 6 do not diminish RNA levels, whereas all but one termination in exons 2 to 5 do (Fig. 7C). None of the mutations creates a nonsense mutation in exon 1, so no conclusions concerning that exon can yet be drawn. Since exon 6 is the final exon of the *dhfr* gene, the natural termination codon is also located in this exon.

Mutant DU8 represents the one apparent exception in this set. In this mutant, the splice site at the 3′ end of exon 2 has been inactivated, and the RNase mapping data suggest that exon 2 is skipped. We have recently examined the *dhfr* mRNA in DU8 by reverse transcribing it into DNA and directly sequencing the DNA after polymerase chain reac-

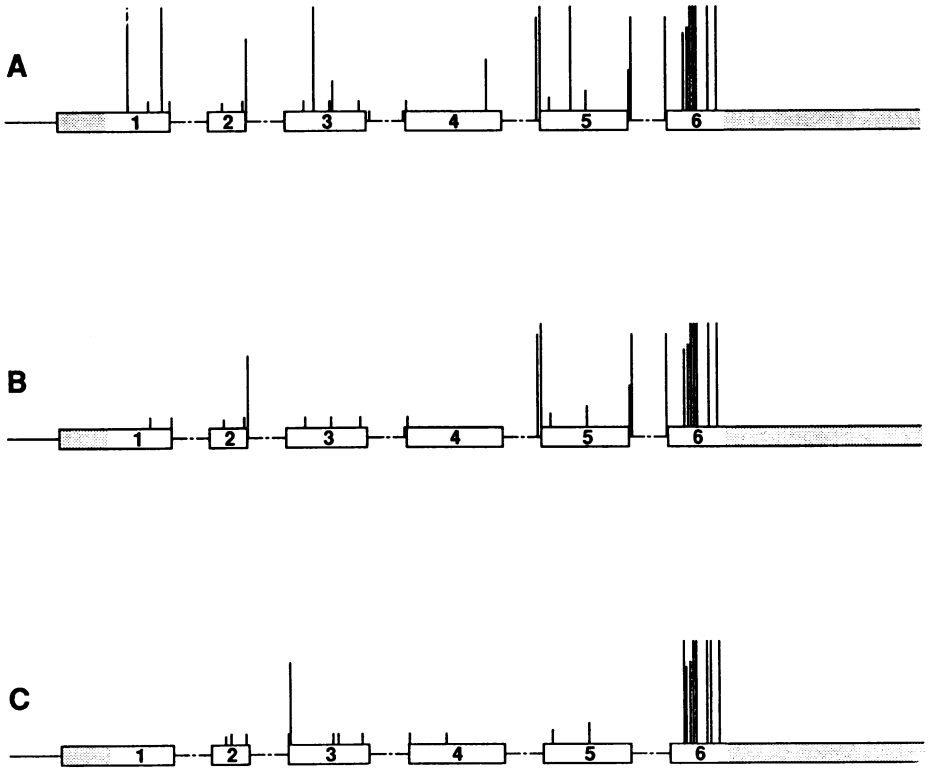

FIG. 7. Map of mutations in the *dhfr* gene and the steady-state amount of *dhfr* mRNA produced. The data are pooled for all mutants whose sequence change has been determined and include spontaneous mutations (41) and mutations induced by benz[*a*]pyrene diol epoxide (9) and by *N*-acetoxy-*N*-acetylaminofluorene (11, 12; Carothers et al., in press) as well as the UV-induced mutations described here. Exons are represented by boxes, with the untranslated parts shaded. Introns (— - —) have been abbreviated. The height of the bar above each exon indicates the relative amount of *dhfr* mRNA determined by RNase protection or Northern analysis. (A) All mutations. (B) Nonsense mutations and nonsense-generating frameshift and splicing mutations. The splicing mutations are those located at the edges of the exons. Note that two of the splicing mutations (at either end of intron 3) result in low RNA levels. (C) Same as panel B except that the positions of the nonsense codons, rather than the mutations themselves, are indicated in the case of frameshift and splicing mutations.

tion amplification (A. M. Carothers, G. Urlaub, J. Mucha, D. Grunberger, and L. A. Chasin, Biotechniques, in press). Exon 1 is indeed spliced to exon 3, creating a frameshift and an opal codon just two bases into exon 3. Since RNA levels are nearly normal in DU8, this mutant represents a deviation from the rule that chain termination codons in exons 2 to 5 result in the low-RNA phenotype. We considered the possibility that protein synthesis may be reinitiated at a downstream ATG in exon 3; however, except for the true initiation codon, no ATG in the coding region is surrounded by the consensus sequence for translation initiation (31). It is interesting to note that the same opal codon at the start of exon 3 is also produced by a frameshift in exon 1 in the case of mutant DU15; this mRNA does contain exon 2, and it is reduced in amount. Thus, the absence of exon 2 seems to suppress the low-RNA phenotype in DU8. Perhaps a rate-limiting step in RNA maturation (e.g., the splicing of intron 1 or 2) is being relieved in mutant DU8, compensating for the negative effects of the generated nonsense codon.

The immunity of exon 6 mutants from the low-RNA phenotype requires a modification of the translational translocation model outlined above. If the rate-limiting step in the transport of pre-mRNA from the nucleus is splicing, then the exceptional status of exon 6 mutations is explained, since by the time a ribosome reaches exon 6, all splicing has been completed. In this model (Fig. 8), the protein synthesis process not only pulls the translating RNA out of the nucleus but also pulls it through the splicing machinery, thus facili-

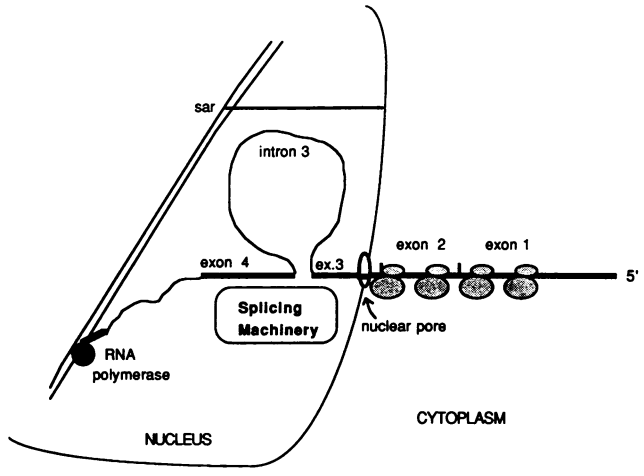

FIG. 8. Translational translocation model for the facilitation of splicing and export of RNA from the nucleus. Ribosomes begin to translate an RNA molecule as it emerges from a nuclear pore. In the course of further translation, the ribosomes pull the transcript through the nuclear pore and through the nuclear splicing machinery as well. Although not essential for the model, transcription of this RNA molecule is shown still in progress, and the transcribed gene is shown positioned near a nuclear pore via attachment of a nuclear scaffold attachment region (sar) to the nuclear lamina.

tating splicing. This idea also explains why the natural chain terminators would not affect RNA levels. Not all RNA molecules would have to participate in this pathway of facilitated processing; thus, the inactivation of this mechanism by premature chain termination reduces, but does not eliminate, mRNA accumulation.

Nuclear scanning of translation frames model. An alternative to the proposition of direct coupling between translation and RNA processing is the existence of a mechanism within the nucleus that scans RNA molecules for the presence of nonsense codons. Such a mechanism would necessarily require that the reading frame of a mRNA precursor be recognized, and so at least one step in RNA processing would have a 5′-to-3′ directionality. Such scanning could be carried out by ribosomelike molecules in the nucleus, perhaps ribosome precursors, or by spliceosomes themselves. It is difficult to justify the evolution of such an elaborate redundancy unless it is part of the very mechanism by which exons are recognized. The process by which the splicing machinery recognizes exons is not yet understood. More than just consensus splice sequences must be recognized in order to avoid cryptic splice sites and to join the appropriate exons to each other. Reading frame information could be used to help define internal exons as regions having acceptor and donor sites bounding a sequence free of chain termination codons. Because of their fixed ends and untranslated regions, the first and last exons would be identified by different rules and so would be immune from the consequences of nonsense codon introduction. Genes with introns located upstream or downstream of protein-coding sequences represent exceptions that may have special mechanisms for splicing, or they may in fact be expressed at reduced levels. Finally, it is interesting in this regard that two genetically defined splicing factors in fungal mitochondria are related to translational functions: tyrosyl-tRNA synthetase is a maturation factor for the *cyt-18* gene in *Neurospora crassa* (2), and in yeast cells the MSS116 gene product, necessary for removing several introns of cytochrome *b* and cytochrome *c* oxidase subunit I transcripts, is homologous to the translation initiation factor eIF4A (52).

The relative low-RNA mutant phenotype is not expressed after transfection. An important constraint must be imposed on these models to account for the results of the gene transfer experiments. As it stands, the models explain why nonsense mutations in an intronless minigene would not exhibit the low-RNA phenotype, since both models involve splicing, and no splicing takes place in these transcripts. However, we did expect to reproduce the difference between wild-type and mutant genes when the full genomic version of a gene with a nonsense mutation was used. Yet the nonsense mutant cosmid construct pDU9 yielded *dhfr* mRNA levels equal to that of the wild-type gene in both stably and transiently transfected cells. We attribute this equivalence not to any special RNA-processing capacity of the transfected gene but rather to the failure of the wild-type transfected gene to partake of the facilitated splicing that is part of the translational translocation or nuclear scanning mechanism. That is, it the wild-type, rather than the mutant, phenotype that is not correctly expressed in the transfected cells. This interpretation is supported by the fact that the absolute level of mRNA accumulation, on a per-gene-copy-number basis, is reduced approximately 20-fold in cells stably transfected with the full genomic gene compared with the level produced by the endogenous gene (Fig. 6). There are at least three differences between the exogenous and endogenous genes: the exogenous genes lack flanking sequences beyond 7 kbp at either end of the gene, they initially lack DNA methylation, and they become integrated at positions different from that of the endogenous gene. The implication is that one or more of these factors can play a role in RNA processing. With regard to the last, it is tempting to define "position" here not (or not only) as the position of a gene within the linear DNA sequence of a chromosome but rather as the position of a gene in relation to structural features of the nucleus. There are nuclear scaffold attachment sites in the fourth intron of the *dhfr* gene in CHO cells, and there is some evidence that these sites are attached to the nuclear lamina (29). One can imagine that positioning of the *dhfr* gene close to a nuclear pore (6) may be necessary for the transcript to avail itself of the postulated translational translocation mechanism.

That the mutant phenotype is not reproduced by the transfected genomic gene raises the question of whether any mechanistic conclusions can be drawn from any of the transfection experiments. We believe that lability of mRNA can still be ruled out from these experiments (as well as the actinomycin D experiment), since to conclude otherwise, one would have to invoke a mechanism by which mature cytoplasmic mRNA produced by a transfected gene could be differentiated from that produced by the endogenous gene.

Nonsense mutations in other mammalian genes affect RNA levels. There have been previous reports of nonsense mutations affecting mRNA levels in mammalian cells. Nonsense mutations in the first two exons of the human β-globin gene result in low globin mRNA levels in the erythrocytes of affected individuals (summarized in reference 4). Studies of the transient expression of cloned mutant genes implicated a nuclear processing step here also, since nuclear as well as cytoplasmic RNA was affected and since no decrease in mRNA stability was demonstrable after actinomycin D treatment (28, 54). A nonsense mutation in the human TPI gene also results in low mRNA levels (19). Daar and Maquat (19) extended this observation by introducing nonsense mutations into the cloned TPI gene by using site-directed mutagenesis. The nonsense mutants produced significantly less TPI mRNA than did the wild type in transient transfection experiments; nonsense codons introduced into the final exon (exon 7) failed to cause a decrease in RNA. These authors found no accumulation of nuclear processing intermediates and concluded that nonsense mutations were affecting mRNA stability. However, no direct measurement of mRNA stability was made. It should be noted that in both the β-globin and TPI experiments, the effects of nonsense mutations were generally demonstrable after gene transfer, whereas we failed to observe an effect after stable or transient transfection of *dhfr* genes. However, this apparent discrepancy may be more quantitative than qualitative, since a dramatic difference in the behavior of in situ versus transfected mutant genes has also been noted in the case of a β-globin nonsense mutation. Mutant β-globin RNA was undetectable in reticulocytes of heterozygotes (less than 3% of the wild-type allele) but was depressed only threefold relative to the level of the wild-type gene after transient transfection of HeLa cells (3). Furthermore, in one study, a β-globin gene with a nonsense mutation did behave as *dhfr*, showing no low-RNA phenotype after transient expression despite an extreme deficiency of mRNA in the thallasemic patient (42). Nonsense mutations have also been reported to decrease immunoglobulin mRNA levels in mouse myeloma cells; mutations in or near the last exon had little effect (5). Taken together, these studies indicate that the phenomenon of decreased RNA levels caused by nonsense mutations is

not limited to housekeeping genes, specialized genes, large genes, or genes assayed in cell culture.

The translational translocation model derives some support from the studies of Muralidhar and Johnson (43), who found that inhibition of protein synthesis by amino acid starvation or cycloheximide treatment in mouse 3T6 cells delayed the nuclear processing time for five different RNA molecules (including *dhfr*) by a factor of 5 but had little effect on transcription or mRNA stability. The translational translocation model or the nuclear scanning model would help to explain the extreme preference for the most 5′ J-region donor splice site when multiple J regions are present in a mature immunoglobulin gene (30, 35). Such polarity is seen only when these transcripts are spliced in vivo, and it is not caused (30) by a "first-come, first served" mechanism (1) based on transcriptional order. This polarity could be explained by the involvement of a translational or translation-like component in the splicing process: the "first come, first served" idea would apply to the 5′-to-3′ process of translation rather than transcription.

Both the nuclear scanning and the translational translocation models are speculative at this point. Moreover, our capacity to test these models by genetic manipulation is hampered by our inability to use standard transfections as an experimental tool. The use of targeted recombination (e.g., reference 55) to replace in situ *dhfr* genes may permit some experiments along these lines. The analysis of additional mutations, especially in exon 1, may help to distinguish between the translation translocation and the nuclear scanning models. Finally, in view of the exceptional mutant DU8, we cannot completely rule out a direct role of RNA secondary structure in labilizing these mutant nuclear transcripts. Whatever the ultimate explanation, it seems likely that these low-RNA mutants are harbingers of RNA-processing phenomena yet to be appreciated.

ACKNOWLEDGMENTS

We thank Adelaide Carothers and Steve Mount for stimulating discussions and Didi Robins for the CAT riboprobe construct.

This work was supported by Public Health Service grant GM-22629 from the National Institute of General Medical Sciences.

LITERATURE CITED

1. **Aebi, M., and C. Weissman.** 1987. Precision and orderliness in splicing. Trends Genet. **3**:102–107.
2. **Akins, R. A., and A. M. Lambowitz.** 1987. A protein required for splicing group I introns in Neurospora mitochondria is mitochondrial tyrosyl-tRNA synthetase or a derivative thereof. Cell **50**:331–345.
3. **Atweh, G. F., H. E. Brickner, X.-X. Zhu, H. H. Kazazian, Jr., and B. G. Forget.** 1988. New amber mutation in a β-thalassemic gene with nonmeasurable levels of mutant messenger RNA in vivo. J. Clin. Invest. **82**:557–561.
4. **Baserga, S. J., and E. J. Benz, Jr.** 1988. Nonsense mutations in the human β-globin gene affect mRNA metabolism. Proc. Natl. Acad. Sci. USA **85**:2056–2060.
5. **Baumann, B., M. J. Potash, and G. Kohler.** 1985. Consequences of frameshift mutations at the immunoglobulin heavy chain locus of the mouse. EMBO J. **4**:351–359.
6. **Blobel, G.** 1985. Gene gating: a hypothesis. Proc. Natl. Acad. Sci. USA **82**:8527–8531.
7. **Buchman, A. R., and P. Berg.** 1988. Comparison of intron-dependent and intron-independent gene expression. Mol. Cell. Biol. **8**:4395–4405.
8. **Burgoyne, L. A., M. A. Wagar, and M. R. Atkinson.** 1970. Calcium-dependent priming of DNA synthesis in isolated rat liver nuclei. Biochem. Biophys. Res. Commun. **39**:254–259.
9. **Carothers, A. M., G. Urlaub, L. A. Chasin, and D. Grunberger.** 1988. Mapping and characterization of mutations induced by benz[*a*]pyrene diol epoxide at dihydrofolate reductase locus in CHO cells. Somatic Cell Mol. Genet. **14**:169–183.
10. **Carothers, A. M., G. Urlaub, N. Ellis, and L. A. Chasin.** 1983. Structure of the dihydrofolate reductase gene in Chinese hamster ovary cells. Nucleic Acids Res. **11**:1997–2012.
11. **Carothers, A. M., G. Urlaub, R. W. Steigerwalt, L. A. Chasin, and D. Grunberger.** 1986. Characterization of mutations induced by 2-(N-acetoxy-N-acetyl)aminofluorene in the dihydrofolate reductase gene of cultured hamster cells. Proc. Natl. Acad. Sci. USA **83**:6519–6523.
12. **Carothers, A. M., G. Urlaub, R. W. Steigerwalt, L. A. Chasin, and D. Grunberger.** 1988. Spectrum of N-2-acetylaminofluorene-induced mutations in the dihydrofolate reductase gene of Chinese hamster ovary cells, p. 337–349. *In* C. M. King, L. J. Romano, and D. Schuetzle (ed.), Carcinogenic and mutagenic responses to aromatic amines and nitroarenes. Elsevier Science Publishing, Inc., New York.
13. **Chasin, L. A.** 1986. The dihydrofolate reductase locus, p. 449–488. *In* M. Gottesman (ed.), Molecular cell genetics: the Chinese hamster cell. John Wiley & Sons, Inc., New York.
14. **Chirgwin, J. M., A. E. Przybyla, R. J. MacDonald, and W. J. Rutter.** 1979. Isolation of biologically active ribonucleic acid from sources enriched in ribonuclease. Biochemistry **18**:5294–5299.
15. **Ciudad, C. J., G. Urlaub, and L. A. Chasin.** 1988. Deletion analysis of the Chinese hamster dihydrofolate reductase gene promoter. J. Biol. Chem. **31**:16274–16282.
16. **Clayton, D. F., A. L. Harrelson, and J. E. Darnell, Jr.** 1985. Dependence of liver-specific transcription on tissue organization. Mol. Cell. Biol. **5**:2623–2632.
17. **Courage-Tebbe, U., and B. Kemper.** 1982. Construction of gapped circular DNA from phage M13 by in vitro hybridization. Biochim. Biophys. Acta **697**:1–5.
18. **Crouse, G. F., R. N. McEwan, and M. L. Pearson.** 1983. Expression and amplification of engineered mouse dihydrofolate reductase minigenes. Mol. Cell. Biol. **3**:257–266.
19. **Daar, I. O., and L. E. Maquat.** 1988. Premature translational termination mediates triosephosphate isomerase mRNA degradation. Mol. Cell. Biol. **8**:802–813.
20. **Drobetsky, E. A., A. J. Grosovsky, and B. W. Glickman.** 1987. The specificity of UV-induced mutations at an endogenous locus in mammalian cells. Proc. Natl. Acad. Sci. USA **84**:9103–9107.
21. **Dworetzky, S. J., and C. M. Feldherr.** 1988. Translocation of RNA-coated gold particles through the nuclear pores of oocytes. J. Cell Biol. **106**:575–584.
22. **Dynan, W. S., S. Sazer, R. Tijan, and R. T. Schimke.** 1986. Transcription factor Sp1 recognizes a DNA sequence in the mouse dihydrofolate reductase promoter. Nature (London) **319**:246–248.
23. **Gasser, C. S., C. C. Simonsen, J. W. Schilling, and R. T. Schimke.** 1982. Expression of abbreviated mouse dihydrofolate reductase genes in cultured hamster cells. Proc. Natl. Acad. Sci. USA **79**:6522–6526.
24. **Glazer, P. M., S. N. Sarkar, and W. C. Summer.** 1986. Detection and analysis of UV-induced mutations in mammalian cell DNA using a lambda shuttle vector. Proc. Natl. Acad. Sci. USA **83**:1041–1044.
25. **Gyllenstein, U. B., and H. Ehrlich.** 1988. Generation of single-stranded DNA by the polymerase chain reaction and its application to direct sequencing of the HLA-DQA locus. Proc. Natl. Acad. Sci. USA **85**:7652–7656.
26. **Hauser, J., M. M. Seidman, K. Sidur, and K. Dixon.** 1986. Sequence specificity of point mutations induced during passage of a UV-irradiated shuttle vector plasmid in monkey cells. Mol. Cell. Biol. **6**:277–285.
27. **Hendrickson, S. L., J.-S. R. Wu, and L. F. Johnson.** 1980. Cell cycle regulation of dihydrofolate reductase mRNA metabolism in mouse fibroblasts. Proc. Natl. Acad. Sci. USA **77**:5140–5144.
28. **Humphries, R. K., T. J. Ley, N. P. Anagnou, A. W. Baur, and A. W. Nienhaus.** 1984. β^0-Thalassemia gene: a premature termination codon causes β-mRNA deficiency without affecting cy-

toplasmic β-mRNA stability. Blood **64**:23–32.
29. **Kas, E. K., and L. A. Chasin.** 1987. Anchorage of the Chinese hamster dihydrofolate reductase gene to the nuclear scaffold occurs in an intragenic region. J. Mol. Biol. **198**:677–692.
30. **Kedes, D. H., and J. Steitz.** 1988. Correct in vivo splicing of the mouse immunoglobulin kappa light-chain pre-mRNA is dependent on 5′ splice-site position even in the absence of transcription. Genes Dev. **2**:1448–1459.
31. **Kozak, M.** 1987. An analysis of the 5′-noncoding sequences of 699 vertebrate messenger RNAs. Nucleic Acids Res. **15**:8125–8148.
32. **Kramer, W., V. Drutsa, H.-W. Jansen, B. Kramer, M. Pflugfelder, and H.-J. Fritz.** 1984. The gapped duplex DNA approach to oligonucleotide-directed mutation construction. Nucleic Acids. Res. **12**:9441–9456.
33. **Lebkowski, J. S., S. Clancy, J. H. Miller, and M. P. Calos.** 1985. The lacI shuttle: rapid analysis of the mutagenic specificity of ultraviolet light in human cells. Proc. Natl. Acad. Sci. USA **82**:8606–8610.
34. **Losson, R., and F. Lacroute.** 1979. Interference of nonsense mutations with eukaryotic messenger RNA stability. Proc. Natl. Acad. Sci. USA **76**:5134–5137.
35. **Lowery, D. E., and B. G. Van Ness.** 1988. Comparison of in vitro and in vivo splice site selection in kappa-immunoglubulin precursor mRNA. Mol. Cell. Biol. **8**:2610–2619.
36. **Luskey, M., and M. R. Botchan.** 1984. Characterization of the bovine papilloma virus plasmid maintenance sequences. Cell **36**:391–401.
37. **McKnight, G. S., and R. D. Palmiter.** 1979. Transcriptional regulation of the ovalbumin and conalbumin genes by steroid hormones in chick oviduct. J. Biol. Chem. **254**:9050–9058.
38. **Melera, P. W., J. P. Davide, C. A. Hession, and K. W. Scotto.** 1984. Phenotypic expression in *Escherichia coli* and nucleotide sequence of two Chinese hamster lung cell cDNAs encoding different dihydrofolate reductases. Mol. Cell. Biol. **4**:38–48.
39. **Melton, D. A., P. A. Krieg, M. R. Rebagliatti, T. Maniatis, K. Zinn, and M. R. Green.** 1984. Efficient *in vitro* synthesis of biologically active mRNA and RNA hybridization probes from plasmids containing a bacteriophage SP6 promoter. Nucleic Acids Res. **12**:7035–7056.
40. **Mitchell, P. J., A. M. Carothers, J. H. Han, J. D. Harding, E. Kas, L. Venolia, and L. A. Chasin.** 1986. Multiple transcriptional start sites, DNase I-hypersensitive sites, and an opposite-strand exon in the 5′ region of the CHO *dhfr* gene. Mol. Cell. Biol. **6**:425–440.
41. **Mitchell, P. J., G. Urlaub, and L. A. Chasin.** 1986. Spontaneous splicing mutations at the dihydrofolate reductase locus in Chinese hamster ovary cells. Mol. Cell. Biol. **6**:1926–1935.
42. **Moschonas, N., E. DeBoer, F. G. Grosveld, H. H. M. Dahl, S. Wright, C. K. Shewmaker, and R. A. Flavell.** 1981. Structure and expression of cloned β^0 thallasemic globin gene. Nucleic Acids Res. **9**:4391–4401.
43. **Muralidhar, M. G., and L. F. Johnson.** 1988. Delayed processing/export of messenger RNA under conditions of reduced protein synthesis. J. Cell. Physiol. **135**:115–121.
44. **Myers, R. M., Z. Larin, and T. Maniatis.** 1985. Detection of single base substitutions by ribonuclease cleavage at mismatches in RNA:DNA duplexes. Science **230**:1242–1246.
45. **Nilsson, G., J. G. Belasco, S. N. Cohen, and A. von Gabain.** 1987. Effect of premature termination of translation on mRNA stability depends on the site of ribosome release. Proc. Natl. Acad. Sci. USA **84**:4890–4894.
46. **Orkin, S. H., and S. Goff.** 1981. Nonsense and frame shift mutations in β^0-thalassemia detected in cloned β-globin genes. J. Biol. Chem. **256**:9782–9784.
47. **Orlofsky, A., and L. A. Chasin.** 1985. A domain of methylation change at the albumin locus in rat hepatoma cell variants. Mol. Cell. Biol. **5**:214–225.
48. **Pachter, J. S., T. J. Yen, and D. W. Cleveland.** 1987. Autoregulation of tubulin expression is achieved through specific degradation of polysomal tubulin mRNAs. Cell **51**:283–292.
49. **Peltz, S. W., and J. Ross.** 1987. Autogenous regulation of histone mRNA decay by histone proteins in a cell-free system. Mol. Cell. Biol. **7**:4345–4356.
50. **Saiki, R. K., D. H. Gelfand, S. Stoffel, S. J. Scharf, et al.** 1988. Primer-directed enzymatic amplification of DNA with a thermostable DNA polymerase. Science **239**:487–491.
51. **Sanger, F., S. Nicklen, and A. R. Coulson.** 1977. DNA sequencing with chain-terminating inhibitors. Proc. Natl. Acad. Sci. USA **74**:5463–5466.
52. **Seraphin, B., M. Simon, A. Boulet, and G. Faye.** 1988. Mitochondrial splicing requires a protein from a novel helicase family. Nature (London) **337**:84–87.
53. **Shimada, T., and A. W. Nienhuis.** 1985. Only the promoter region of the constitutively expressed normal and amplified human dihydrofolate reductase gene is DNase I hypersensitive and undermethylated. J. Biol. Chem. **260**:2468–2474.
54. **Takeshita, K., B. G. Forget, A. Scarpa, and E. B. Benz, Jr.** 1984. Intranuclear defect in β-globin mRNA accumulation due to a premature translation termination codon. Blood **84**:13–22.
55. **Thomas, K. R., and M. R. Capecchi.** 1987. Site-directed mutagenesis by gene targeting in mouse embryo-derived stem cells. Cell **51**:503–512.
56. **Unwin, P. N. T., and R. A. Milligan.** 1982. A large particle associated with the perimeter of the nuclear pore complex. J. Cell Biol. **93**:63–75.
57. **Urlaub, G., A. M. Carothers, and L. A. Chasin.** 1985. Efficient cloning of single copy genes using specialized cosmid vectors: isolation of mutant dihydrofolate reductase genes. Proc. Natl. Acad. Sci. USA **82**:1189–1193.
58. **Urlaub, G., and L. A. Chasin.** 1980. Isolation of Chinese hamster cell mutants deficient in dihydrofolate reductase activity. Proc. Natl. Acad. Sci. USA **77**:4216–4220.
59. **Urlaub, G., E. Kas, A. M. Carothers, and L. A. Chasin.** 1983. Deletion of the diploid dihydrofolate reductase locus from cultured mammalian cells. Cell **33**:405–412.
60. **Urlaub, G., M. Landzberg, and L. A. Chasin.** 1981. Selective killing of methotrexate-resistant cells: segregation of dihydrofolate reductase genes. Cancer Res. **41**:1594–1601.
61. **Urlaub, G., P. J. Mitchell, E. Kas, V. L. Funanage, T. T. Myoda, and J. L. Hamlin.** 1986. Effect of gamma rays at the dihydrofolate reductase locus: deletions and inversions. Somatic Cell Mol. Genet. **12**:555–566.
62. **Venolia, L., G. Urlaub, and L. A. Chasin.** 1987. Polyadenylation of Chinese hamster dihydrofolate reductase genomic genes and minigenes after gene transfer. Somatic Cell Mol. Genet. **13**:491–501.
63. **Wigler, M., A. Pellicer, S. Silverstein, R. Axel, G. Urlaub, and L. A. Chasin.** 1979. Transformation of the APRT locus in mammalian cells. Proc. Natl. Acad. Sci. USA **76**:1373–1376.
64. **Winter, E., F. Yamamoto, C. Almoguera, and M. Perucho.** 1985. A method to detect and characterize point mutations in transcribed genes: amplification and overexpression of the mutant c-Ki-ras allele in human tumor cells. Proc. Natl. Acad. Sci. USA **82**:7575–7579.
65. **Zasloff, M.** 1983. tRNA transport from the nucleus in a eukaryotic cell: carrier-mediated translocation process. Proc. Natl. Acad. Sci. USA **80**:6436–6440.